Experimental evidence of self-excited relaxation oscillations leading to homoclinic behavior in spreading flames

P. L. García-Ybarra, J. C. Antoranz, V. Sankovitch, and J. L. Castillo
Departamento de Física Fundamental, Laboratoire de Combustión y Digitalización de Imágenes, Universidad Nacional de Educación a Distancia, Apartado 60141, 28080 Madrid, Spain
(Received 3 November 1993; revised manuscript received 9 February 1994)

Flame spreading over liquid alcohols has been experimentally characterized by three methods: temperature measurements along the liquid surface, schlieren pictures of the temperature gradients induced in the liquid by Marangoni flows, and direct video recording of the flame spreading. Three distinct spreading regimes have been observed: a fast and a slow propagation regime of uniform spreading at high and low values of the initial fuel surface temperature, and an oscillatory propagation regime at intermediate temperatures. The oscillations start as a Hopf bifurcation from the fast propagation steady state. Moreover, the collision of the limit cycle with the slow spreading branch originates a homoclinic connection revealed by a logarithmic divergence in the oscillation period, a main feature of generic homoclinic points.

PACS number(s): 47.70.Fw, 47.20.Ky, 47.20.Dr, 82.40.Py

INTRODUCTION

Relaxation oscillations in well-stirred chemical reactors have been observed and modeled since more than twenty years ago [1]. At about the same time, oscillations were also reported to occur by Akita [2] in a different kind of chemically reacting system, namely in the propagation velocity of a flame spreading over a liquid fuel. Since then, whereas the oscillations in stirred reactors have become a recurrent topic in the study of complex systems exhibiting low dimensional dynamical behavior [3], the oscillatory flame spreading observed by Akita has not been recognized as belonging to the same class of systems and then, has not been considered from the view point of the proper framework. Only very recently, experiments conducted in nonhomogeneous reactors have opened an experimental way along this direction [4]. Unlike a homogeneous reaction system, flame spreading above a condensed fuel is an example of a propagating chemical reaction front. The propagation velocity is self-adjusted according to the prevailing energetic and fuel availability conditions, in such a way that diffusion and convection of heat and of chemical species are essential parts of the control mechanisms.

The spreading of a flame over a liquid fuel layer presents several well-differentiated regimes [2,5], depending on the initial liquid surface temperature, T_∞. For temperatures higher than the flash point temperature, T_{FP}, the flame can propagate in the gas phase without additional fuel intake from the liquid phase. However, for liquid temperatures lower than T_{FP}, the flame spreading depends strongly on the interaction between the flame and the liquid. The flame needs to heat up the liquid underneath, in order to increase the equilibrium vapor pressure and as a consequence the amount of fuel available in the gas phase. This addition of fuel brings the gaseous mixture within the lean flammability limit that allows the flame propagation. Moreover, the nonuniform heating of the liquid can generate surface motions *via* Marangoni effect (the surface traction induced in a liquid layer due to the presence of a temperature gradient along the surface) which penetrate in the liquid bulk by viscous stresses. Figure 1 is a sketch of the flame spreading in the reactive gas phase with a constant velocity, v_f, over a liquid fuel. The local heating of the liquid surface may induce a vortex on the liquid layer. In the steady regimes, the vortex moves attached to the flame front. Contrasted with flame spreading above a solid fuel, the appearance of Marangoni flows is a distinctive characteristic of flame spreading above liquids and provides the necessary mechanism for the oscillatory spreading. Different opinions have been manifested on the nature of this oscillatory behavior but none of the presented models gives a comprehensive explanation of the whole phenomenon [2,6–8]. Very recently, a numerical integration of the corresponding two dimensional problem was performed [9] where oscillatory spreading was attributed to

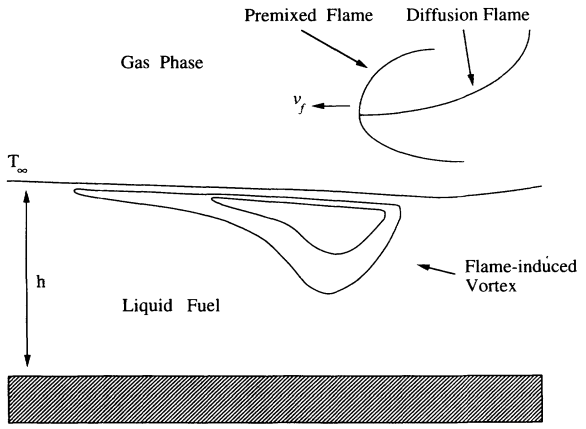

FIG. 1. Sketch of a steadily spreading flame with a Marangoni vortex induced in the liquid layer.

the complex flow pattern induced in the gas phase.

At present, the following facts seem to be well established for flames spreading over liquid alcohols filling thin channels (narrowed to soften three dimensional effects): at the higher temperatures ($T_{FP} \approx T_\infty > T_{osc}$), the induced motions in the liquid are of small scale (≈ 0.1 cm) and help the flame to spread steadily with a high velocity ($\approx 10^2$ to 10 cm/s) [10]. In the other extreme, for sufficiently low liquid temperatures, $T_\infty < T_H$, the generated motions in the liquid are of large scale (≈ 10 cm). Flame spreading is also uniform but the flame goes on at a much lower speed (≈ 1 cm/s) and it is preceded by an elongated vortex in the liquid. In the intermediate temperature range, $T_{osc} > T_\infty > T_H$, the flame shows oscillatory behavior [2,6,7], with a spreading velocity that remains low most of the time, but alternates with spikes of fast propagation.

To study experimentally the regimes of flame spreading below T_{FP} and the characteristics of the transitions between the different regimes, we have performed a series of experiments on flame spreading above liquid alcohols (methanol, ethanol, isopropanol, and *n*-butanol). The experiments were carried out using the experimental device depicted in the following section. There, the implemented measurement techniques are also indicated. Then, a description of the main experimental flame spreading features in terms of these measurements is given. Right after, these results are discussed and interpreted, to end up with a summary of the outstanding conclusions.

EXPERIMENTAL SETUP AND MEASUREMENTS

The experiments were conducted in an open channel configuration with the arrangement shown in Fig. 2. The channel was 2.5 cm wide, 40 cm long, and 4 cm deep, made in aluminum and thermalized by the flow of a liquid coolant along an U-shaped tube at the bottom. Two thick Pyrex windows (10 cm long), centered along the lateral walls, one on each side of the container, allowed the optical access to the fuel layer. The gas mixture was ignited at one end of the channel and the spreading observed until the flame reached the other end. Three techniques were set up to analyze the flame spreading (see Fig. 2): (i) liquid temperatures were measured and controlled by inserting an array of eight Cr-Al thermocouples (diameter of 25 μm) disposed on the fuel surface at regular intervals of 2 cm along the channel (maximum sampling rate was 1 kHz); (ii) a classical Teopler schlieren system was used to visualize the large temperature gradients established in the liquid by the intermixing of hot and cold liquid in the Marangoni vortex ahead of the flame, and the pictures through the Pyrex windows were recorded with a video camera (25 frames/s); and (iii) The spreading of the flame was directly recorded with another video camera.

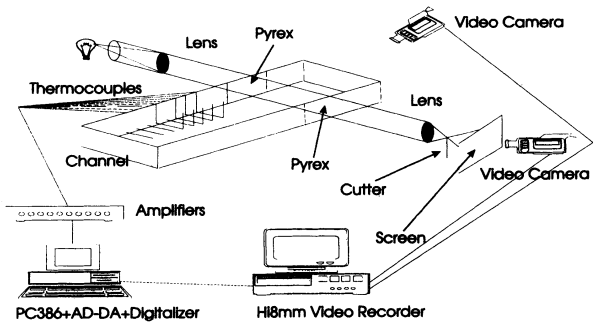

FIG. 2. Scheme of the measurement techniques used in the experiments. AD-DA stands for analog to digital and digital to analog input/output board.

From the thermocouple readings, the arrival of the flame to each thermocouple location is easily detected. That provides the average spreading velocity between thermocouples (this method of measurement is specially suitable for fast steady propagation regimes due to the high frequency of sampling). Also, from the direct video recording and, after an image analysis, a measure of the spreading velocity, v_f, can be made at any location along the channel. With all this information, the maximum, the minimum, and the mean spreading velocity of the flame can be represented as a function of the initial liquid surface temperature, T_∞. The diagram for isopropanol is depicted in Fig. 3. Squares represent the maximum measured spreading velocity for the given temperature T_∞, circles correspond to the minimum observed v_f, and rhombi are the mean spreading velocities. The three mentioned spreading regimes are clearly differentiated. For temperatures $T_\infty > T_{osc}$ (respectively, $T_\infty < T_H$), *fast* (respectively, *slow*) steady-state spreading regimes are observed. For these temperature ranges, there are no significant differences between the maximum and the minimum spreading velocities. However, for intermediate temperatures, $T_H < T_\infty < T_{osc}$, the flame exhibits oscillatory behavior. The limit cycle regime is born, at $T_\infty = T_{osc}$, as a Hopf bifurcation from the *fast* spreading regime and finishes suddenly at $T_\infty = T_H$ when the slow spreading regime establishes.

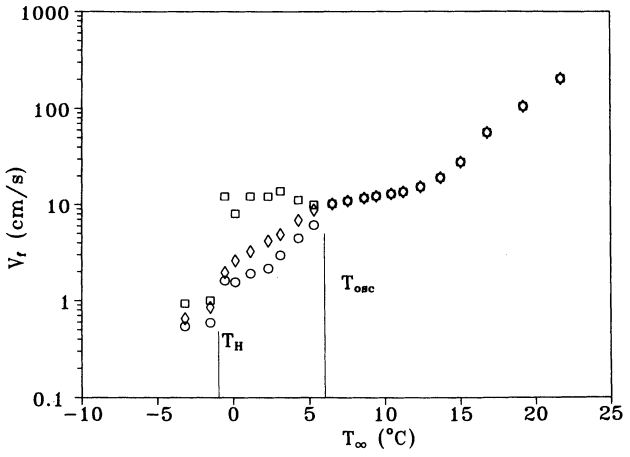

FIG. 3. Bifurcation diagram showing the spreading flame velocity, v_f, *versus* the initial surface temperature, T_∞ for isopropanol. Squares denote the maximum velocity, circles are the minimum velocity, and rhombi depict the mean velocity.

The schlieren pictures and the thermocouple records do not detect any Marangoni circulation zone, preceding the flame, in the *fast* propagation regime. However, the schlieren image, in the very vicinity of the surface, is blackened by the liquid meniscus at the Pyrex windows. The thickness of the blackened region is of the order of one-tenth of the centimeter. On the other hand, the thermocouples do not show any increase in the liquid temperature until the luminous zone of the flame appears to be over them. These two observations suggest that, in this case, the Marangoni vortex should have a characteristic length of the order of 0.1 cm or even smaller. During the *slow* propagation regime, on the contrary, a large vortex in the liquid ahead of the flame is clearly present. For the lower temperatures the vortex even reaches the size of the container and the presence of the end wall influences our measurements. Lastly, the preceding Marangoni vortex periodically appears and disappears in the oscillatory regime.

DISCUSSION AND INTERPRETATION OF RESULTS

Flame spreading can be explained by the propagation of a tiny premixed flame trailing behind a long diffusion flame where the vaporized fuel burns up (see the sketch shown in Fig. 1). This peculiar structure is known as a triple flame [11,12]. For liquid fuels, the qualitative features of the steady state flame spreading driven by Marangoni effect are described in [5]. Both the triple flame and the Marangoni vortex possess very complex structures that have prevented, to date, the theoretical account of their coupling. The vortex induced in the liquid fuel, ahead of the flame, brings hot liquid from the region under the flame edge and generates a substantial increase of the surface temperature on the affected region. Besides, in the gas phase, another vortex is build up with an enriched (and overheated) gas reactive mixture that assists the combustion process by slowing down the associated chemical reaction time. When the initial fuel temperature is decreased, the flame propagation velocity diminishes and the vortex size enlarges as well as its characteristic time. The oscillatory behavior appears when this time becomes larger than the characteristic transit time of the flame along the vortex length. Then, the vortex structure is unable to follow the flame advancement. The flame goes on quickly through the enriched gas mixture up to approaching the border of the vortex where the preceding conditions (leaner and colder mixture) increase the combustion time. As the flame reduces its propagation velocity, Marangoni effect is able to rebuild a new vortex that, after some induction time, affects the flame by reducing the combustion time. Then, the flame accelerates again and the process restarts.

The preceding discussion indicates that instead of using the initial surface temperature (that is not a variable), it seems more appropriate to use the temperature on the surface ahead of the flame as the temperature controlling the flame spreading. The trajectories of the system in phase space can be projected onto the plane T_S, v_f.

For the *fast* propagation regimes, the surface and the initial bulk temperatures coincide (within the experimental resolution), but in the *slow* propagation regimes the temperature in the recirculation zone, over the liquid surface, increases from the vortex edge until it reaches an almost plateau value and then suddenly increases again when the flame arrives. We can use the maximum value at the plateau as the effective surface temperature T_S. In Fig. 4, the flame spreading velocity is plotted against this effective liquid surface temperature, T_S, for isopropanol. The *fast* propagation branch is depicted with squares and it is exactly the same as in Fig. 3. The *slow* steady propagation corresponds to the line joining the circles. Both steady propagation modes overlap in a *bistable* zone whose width increases with the fuel molecular weight, ranging from 2–10°C, respectively, for the methanol and the *n*-butanol. Although the word *bistable* is not properly used (because the overlapping states correspond, in fact, to different values of the control parameter, T_∞) Fig. 4 provides an easy interpretation of the limit cycle behavior as the occurrence of relaxation oscillations around this *bistability* region, self-excited by the coupling with the Marangoni effect that provides oscillating values for T_S. Figure 4 includes also the approximate projections of two limit cycle orbits, obtained by interpolating data from the thermocouples and the video records. The dashed orbit represents the trajectory of the flame velocity and surface temperature along the limit cycle, for $T_\infty = 3.1\,^\circ\mathrm{C}$, well within the *bistable* region. The solid limit circle depicts the same information for $T_\infty = -0.5\,^\circ\mathrm{C}$, very near the disappearance of the oscillations. The flame spends most of the time around the region of lower velocities and the limit cycle disappears

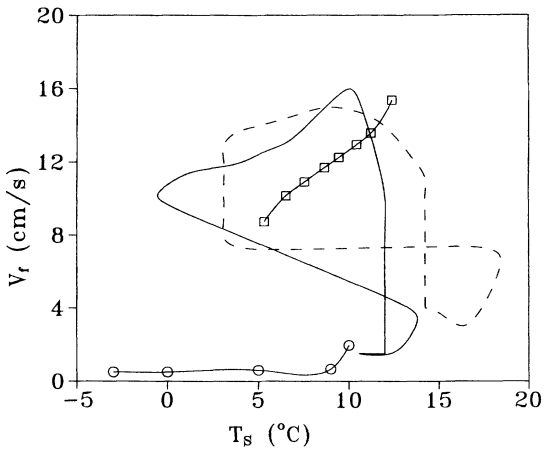

FIG. 4. Bifurcation diagram showing the spreading flame velocity, v_f, *versus* the effective surface temperature, T_S for isopropanol. The branch joining the squares corresponds to the *fast* propagation regime, whereas the lower branch with the circles represents the states of steady *slow* propagation. Also the approximated projections of the trajectories during two oscillatory regimes are plotted. The dashed orbit is for $T_\infty = 3.1\,^\circ\mathrm{C}$ and the solid limit cycle depicts the trajectory for $T_\infty = -0.5\,^\circ\mathrm{C}$.

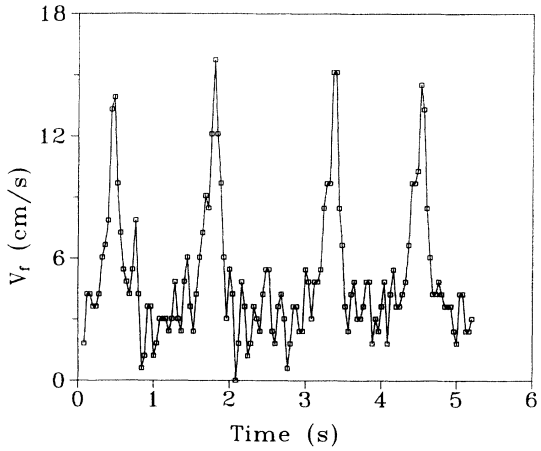

FIG. 5. Flame velocity versus time for isopropanol at $T_\infty = 3.1\,^\circ$C. Time interval between points is 40 ms.

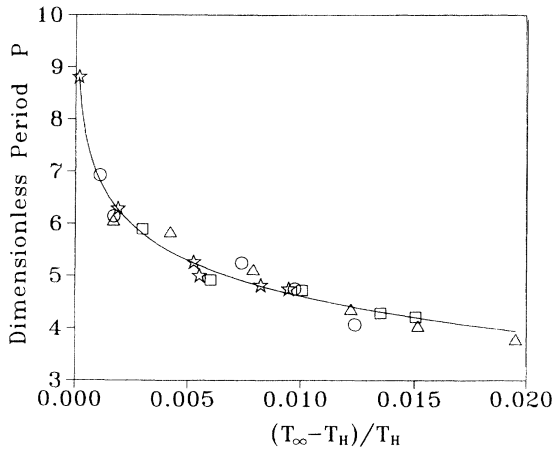

FIG. 6. Dimensionless period of oscillations versus dimensionless distance to the homoclinic bifurcation point for different alcohols. Stars denote methanol, squares ethanol, triangles isopropanol, and circles n-butanol. The solid line is the theoretical divergence for a generic homoclinic point represented by $P = -\ln[(T_\infty - T_H)/T_H]$.

when it touches the branch of *slow* propagation. The oscillations in the spreading velocity corresponding to the first orbit ($T_\infty = 3.1\,^\circ$C) are depicted in Fig. 5. The flame exhibits most of the time a low propagation speed but presents periodical bursts of very rapid propagation.

At the temperature T_H, the limit cycle collides with a steady state. Therefore, T_H corresponds to a homoclinic point. The oscillation period has to be identified with the induction time required for the fast propagation burst to occur. A divergence in this induction time (hence in the oscillation period) should be expected close to the conditions where the slow propagation regime is definitely established. The divergence is logarithmic for a generic homoclinic point [13]. In order to obtain the features of our homoclinic point, we have approximated the observed divergence in the period of the oscillations by a logarithmic fit. The homoclinic temperature was obtained for each alcohol using the data similar to the ones depicted in Fig. 3. Then, the measured period, τ was related to the relative distance to the homoclinic temperature, $(T_\infty - T_H)/T_H$, by the expression $\tau = a - b\ln[(T_\infty - T_H)/T_H]$, with T in kelvin. The dimensionless period $P = (\tau - a)/b$ is plotted in Fig. 6, where stars, squares, triangles, and circles stand for methanol, ethanol, isopropanol, and n-butanol, respectively. There exists a satisfactory fit of the measured oscillation periods with a logarithmic divergence law, $-\ln[(T_\infty - T_H)/T_H]$, represented by the solid curve. The discrepancies between our data and the theoretical curve are well within the experimental error.

CONCLUSIONS

The transitions between the different regimes of flame spreading over liquid fuels have been experimentally characterized. By decreasing the control parameter value (initial surface temperature, T_∞), a sequence of different flame spreading regimes is observed, evolving from a fast steady state, to a limit cycle and, later on to a new steady state of slow flame propagation. The uniform spreading observed at high fuel temperatures becomes unstable and an oscillatory state originates via a Hopf bifurcation at a critical value of the initial surface temperature, $T_{\infty,c1} = T_{\rm osc}$. Along this limit cycle, the spreading velocity varies between two extreme positive values. Far away from this bifurcation point, the oscillation adopts the characteristics of a relaxation oscillation: the flame propagates with the slow velocity most of the time but presents sharp spikes of the fast spreading. By decreasing even further the surface temperature, the size of the limit cycle increases until it collides with the homoclinic orbit. This collision determines a homoclinic point which appears at $T_{\infty,c2} = T_H < T_{\rm osc}$. For even lower surface temperatures a new stable steady state of slow propagation is definitively established. Figure 3 shows an experimental bifurcation diagram where the initial fuel temperature, T_∞, is the control parameter. It is worthwhile to notice the similarity between this bifurcation sequence and the sequence obtained numerically from a five-equations simplified model which simulates the behavior of a laser with saturable absorber [14]. In the laser, the Q-switching oscillatory regime ends in a homoclinic orbit with an infinite period, and then the system moves to a steady state. Such a reduced model is still unknown for the phenomenon of flame spreading but the reported experimental findings support the idea of its existence and open the way to a theoretical study along this direction. New experiments are actually under way using a longer spreading channel to look for possible finite box effects on the bifurcation sequence. The results will be reported elsewhere.

ACKNOWLEDGMENTS

This work was supported by the Dirección General de Investigación Científica y Técnica (DGICYT, Spanish Ministry of Education and Science) under Project No. PB91-0221 and by the Madrid Community Government under Contract No. CAM-E158-92.

[1] B. H. Lavenda, G. Nicolis, and M. Herschkowitz-Kaufman, J. Theor. Biol. **32**, 283 (1971).

[2] K. Akita, in *Proceedings of the Fourteenth Symposium (International) on Combustion, University Park, PA, 1972* (The Combustion Institute, Pittsburgh, PA, 1973), p. 1075.

[3] R. Serra, M. Andretta, G. Zanarini, and M. Compiani, *Introduction to the Physics of Complex Systems* (Pergamon, Oxford, 1986).

[4] See, for instance, the related works collected in *Nonlinear Wave Processes in Excitable Media*, Vol. 244 of *NATO Advanced Study Institute, Series B: Physics*, edited by A. V. Holden, M. Markus, and H. G. Othmer (Plenum, New York, 1991).

[5] F. A. Williams, *Combustion Theory* (Benjamin/Cummings, Menlo Park, CA, 1985), 2nd ed.

[6] R. Mackinven, J. Hansel, and I. Glassman, Comb. Sci. Tech. **1**, 293 (1970).

[7] A. Ito, D. Masuda, and K. Saito, Combust. Flame **83**, 375 (1991).

[8] I. Glassman and F. L. Dryer, Fire Safety J. **3**, 123 (1980).

[9] C. Di Blasi, S. Crescitelli, and G. Russo, in *Proceedings of the Twenty-Third Symposium (International) on Combustion, Orléans, France, 1990* (The Combustion Institute, Pittsburgh, PA, 1991), p. 1669.

[10] M. Furuta, J. Humphrey, and A. C. Fernandez-Pello, Phys. Chem. Hydrodynamics **6**, 355 (1985).

[11] J. W. Dold, Combust. Flame **76**, 71 (1989).

[12] A. Liñán, *Combustion in High Speed Flows*, edited by J. D. Buckmaster, T. L. Jackson, and A. Kumar (Kluwer, Dordrecht, in press).

[13] C. Kaas-Petersen and S. K. Scott, Physica D **32**, 461 (1993). For more details on homoclinic behavior see Physica D **62** (1993); the whole volume is devoted to this topic.

[14] J.C. Antoranz, J. Gea, and M. G. Velarde, Phys. Rev. Lett. **47**, 1895 (1981) and J. C. Antoranz, L. L. Bonilla, J. Gea, and M. G. Velarde, *ibid.* **49**, 35 (1982).